scientific reports

OPEN

Automated diagnosis for extraction difficulty of maxillary and mandibular third molars and post-extraction complications using deep learning

Junseok Lee[1], Jumi Park[2], Seongju Lee[1], Seong-Yong Moon[3] & Kyoobin Lee[1]✉

Optimal surgical methods require accurate prediction of extraction difficulty and complications. Although various automated methods related to third molar (M3) extraction have been proposed, none fully predict both extraction difficulty and post-extraction complications. This study proposes an automatic diagnosis method based on state-of-the-art semantic segmentation and classification models to predict the extraction difficulty of maxillary and mandibular M3s and possible complications (sinus perforation and inferior alveolar nerve (IAN) injury). A dataset of 4,903 orthopantomographys (OPGs), annotated by experts, was used. The proposed diagnosis method segments M3s (#18, #28, #38, #48), second molars (#17, #27, #37, #47), maxillary sinuses, and inferior alveolar canal (IAC) in OPGs using a segmentation model and extracts the region of interest (RoI). Using the RoI as input, the classification model predicts extraction difficulty and complication possibilities. The model achieved 87.97% and 88.85% accuracy in predicting maxillary and mandibular M3 extraction difficulty, with area under the receiver operating characteristic curve (AUROC) of 96.25% and 97.3%, respectively. It also predicted the possibility of sinus perforation and IAN injury with 91.45% and 88.47% accuracy, and AUROC of 91.78% and 94.13%, respectively. Our results show that the proposed method effectively predicts the extraction difficulty and complications of maxillary and mandibular M3s using OPG, and could serve as a decision support system for clinicians before surgery.

Keywords Extraction difficulty, Deep learning, Orthopantomographys, Post-extraction complications, Third molar

The extraction of third molars (M3) is a common procedure in oral and maxillofacial surgery, experienced by approximately 30–60% of people[1–3]. Since M3 grows at different angles and positions in each person, an accurate diagnosis tailored to each person is crucial. Especially because complications like inferior alveolar nerve (IAN) injury and sinus perforation, which can be serious for patients, may occur after maxillary and mandibular M3 extraction[4–7]. IAN injury can cause sensory impairment and speech and chewing difficulties[8,9]. Sinus perforation, which occurs due to the postnasal drainage of secretions, can cause coughing and halitosis, reduced sense of taste and smell, and pain in the upper teeth area[10].

A orthopantomography (OPG) is a primary diagnostic tool for various dental diseases. Dentists analyze the extraction difficulty and possibility of complications based on various oral factors, such as M3 s, second molars, maxillary sinus, and inferior alveolar canal (IAC), in OPG. Several signs can diagnose the extraction difficulty and possibility of sinus perforation and IAN injury. The extraction difficulty is determined according to the depth and angulation of the impacted M3[11–13]. Furthermore, the possibility of IAN injury or sinus perforation can be predicted through the correlation between the mandibular M3 and IAN and the maxillary M3 and maxillary sinus, respectively[5,6].

Deep learning has improved the performance of classification, detection, and segmentation tasks in various fields[14–16,22,33]. Studies have been proposed to predict the extraction difficulty of M3 s and the relationships between mandibular M3 s and the IAC, and maxillary M3 s and sinus in orthopantomography using deep

[1]Department of AI Convergence, Gwangju Institute of Science and Technology (GIST), Gwangju, Republic of Korea. [2]Naval R&D Center, Hanwha systems, Seoul, Gyeonggi-Do, Republic of Korea. [3]Department of Oral and Maxillofacial Surgery, College of Dentistry, Chosun University, Gwangju, Republic of Korea. ✉email: kyoobinlee@gist.ac.kr

learning[17–21]. Torul et al. proposed a method to predict the extraction difficulty of maxillary M3 s and the relationship between the maxillary M3 and the sinus[18]. Soltani et al. proposed a study to detect mandibular M3 and IAC, and classify their relationship as contact or non-contact[19]. Trachoo et al. proposed a method for classifying the extraction difficulty of mandibular M3 s, but it has an inefficient structure by splitting the orthopantomography and adding a model to predict the right and left sides[20]. Kumbasar et al. proposed a method for classifying the spatial relationship between the mandibular M3 and the IAC, but it is not fully automated because it requires manual cropping of the M3 region[21]. Most previous studies use bounding boxes to detect the position of M3 s in orthopantomography and perform classification based on the detected M3 s. However, these studies overlook the use of segmentation models, which can detect the M3 position and provide semantic mask that offer valuable hints for classification. Also, studies are limited as they only address partial functionalities. In real-world scenarios, a method that predicts the extraction difficulty of both maxillary and mandibular third molars and their relationships to the maxillary sinus and IAC is essential.

This study proposes a novel deep learning method for simultaneous and fully automatic prediction of the extraction difficulty and possible complications for the maxillary and mandibular M3 s. The proposed method segments the M3 s, second molars, maxillary sinus, and IAC from OPG, and classifies the extraction difficulty of the maxillary and mandibular M3 s and the potential possibility of maxillary perforation and IAN injury after extraction. Furthermore, we used a semantic mask generated through a segmentation model as input to the classification model with a OPG to enhance the classification performance, as shown in Fig. 1.

The aim of this study is to develop a suitable deep learning model to predict the extraction difficulty and potential complications of both maxillary and mandibular M3 s using OPGs before surgery. This system is expected to be used as a diagnostic support tool for clinicians.

Materials and methods

Dataset information

This study was approved by the Institutional Review Boards of the Gwangju Institute of Science and Technology (20210217-HR-59-01-02) and the Chosun University Dental Hospital (CUDHIRB 2005008). This study was a retrospective study, for which the requirement for informed consent was waived by the Institutional Review Board of Gwangju Institute of Science and Technology and Chosun University Dental Hospital due to its data

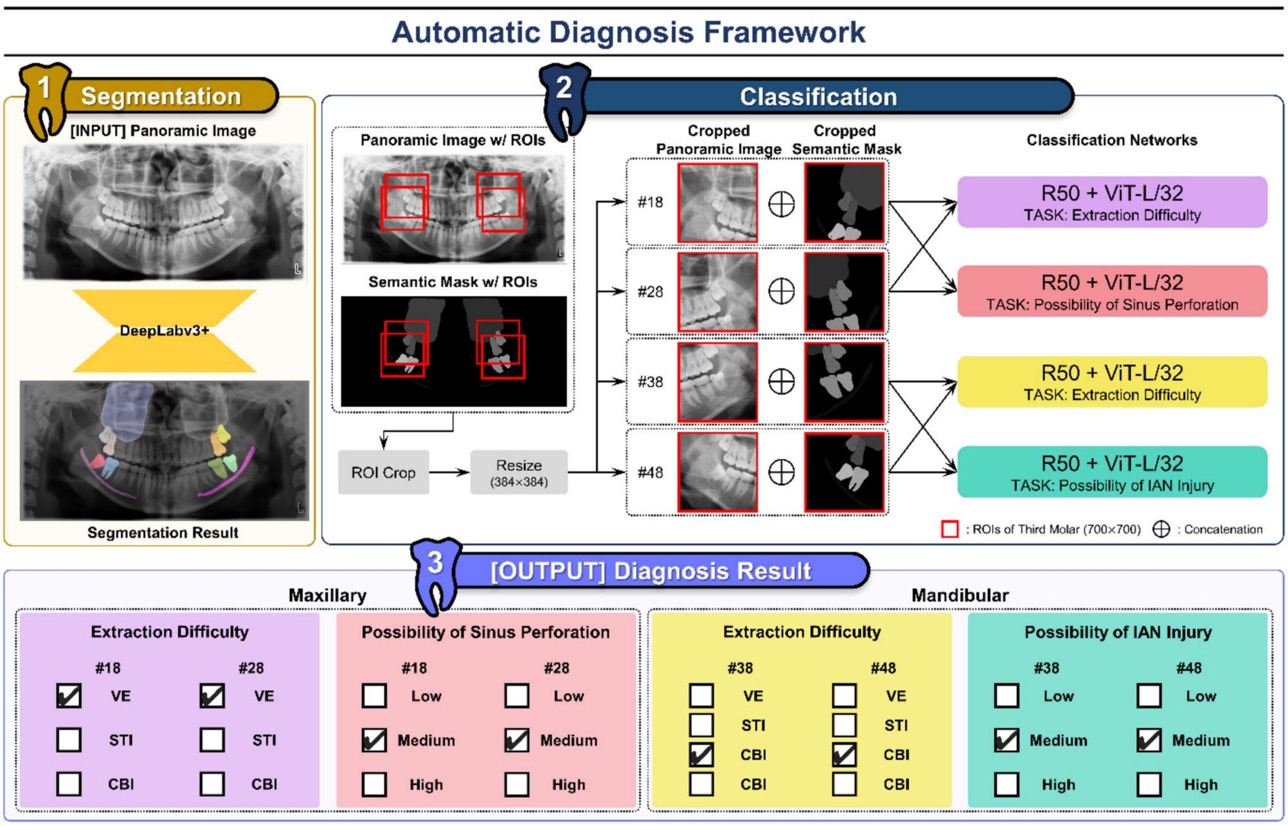

Fig. 1. Overall framework for the diagnosis of extraction difficulty and complications. **(Segmentation)** DeepLabv3 + segments the third molars, second molars, maxillary sinuses, and IACs in the panoramic image. The red box is the RoI of 700 × 700 size with maxillary third molar (#18). **(Classification)** The RoI of the panoramic image and the semantic mask are concatenated and used as inputs to the R50 + Vision Transformer to classify extraction difficulty and complications. **(Diagnosis Result)** Diagnosis result of the extraction difficulty and possibility of complications of third molars (#18, #28, #38, #48).

source and methods. The dataset collection and experiments were performed in accordance with the approved ethical guidelines and regulations. The dataset consists of 4,903 OPGs acquired through eight panoramic photography devices manufactured by Planmeca, Vatech, HDXWILL, Pointnix, and Gendex. The OPGs varied based on myriad factors such as resolution, sharpness, contrast, and brightness due to different manufacturers. OPGs were approximately 1,300 × 800 to 3,000 × 1,500 in size. To evaluate the model's generalization ability, the dataset was randomly split into training, validation, and testing sets. The dataset was divided in the ratio of 3,376 for training, 476 for validation, and 1,051 for testing.

Segmentation and classification labels

For training deep learning models, 4,903 OPGs were annotated by seven dentists. For the segmentation model, each OPG was considered for 13 classes, which included M3 s (#18, #28, #38, #48), second molars (#17, #27, #37, #47), maxillary sinus (left and right), IAC (left and right), and the background of the image.

For the classification model, 6,356 maxillary M3 s were labeled for extraction difficulty and sinus perforation, and 8,716 mandibular M3 s were labeled for extraction difficulty and IAN injury. Table 1shows the number of M3 s labeled for each class. According to Pell & Gregory and Winter's classifications, the extraction difficulty of the maxillary and mandibular is determined based on the combination of the impaction type of the maxillary and mandibular M3[26,27,37,38]. Each impaction type is shown in Fig. 2. According to clinical procedure, extraction difficulty can be divided into four categories: vertical eruption (VE), soft tissue impaction (STI), partial bony impaction (PBI), and complete bony impaction (CBI). VE means a simple extraction method without gum incision or bone fracture. STI means an extraction method after gum incision. PBI requires tooth partition for extraction. CBI requires tooth partition and bone fracture when more than 2/3 of the crown is impacted. Since the maxillary M3 is rarely diagnosed with PBI, there are no PBI cases in our dataset. Therefore, we divide the extraction difficulty into VE, STI, and CBI. Depending on the depth of the impacted maxillary M3, impaction types can be classified as A, B, and C classes. Moreover, depending on the angle of the impacted maxillary M3, there are six types of impaction: vertical (10 ° to − 10 °), mesioangular (11 ° to 79 °), horizontal (80 ° to 100 °), distoangular (− 11 ° to − 79 °), transverse (buccal-lingual), and inverted (101 ° to − 80 °). As shown in Table 2, extraction difficulty is determined as VE, STI, or CBI, depending on the depth and angle of the impacted maxillary M3. The mandibular M3 is classified A, B, and C according to the impacted depth and class I, class II, and class III according to the distance between the mandibular M3 and the ascending mandibular ramus. Likewise, the mandibular M3 is classified into six types depending on the angle of the impacted mandibular M3. The extraction difficulty of the mandibular M3 is determined by a combination of classes A, B, and C and classes I, II, and III, as well as the angle of the impacted mandibular M3, as shown in Table 3.

Sinus perforation possibility (low, medium, high) is determined by how close the maxillary M3 root is to the maxillary sinus. Sinus perforation is classified as low, medium, and high depending on wheter the root of the maxillary M3 does not reach the maxillary sinus, reaches the maxillary sinus, and penetrates the maxillary sinus. IAN injury is determined by the relative position of the impacted mandibular M3 with the IAC. Therefore, IAN injury is classified as low if the root of the mandibular M3 does not reach the IAC, medium if it interrupts the upper boundary of the IAC, and high if it interrupts both the upper and lower boundaries of the IAC.

Characteristic	Train (n = 3,376)	Val (n = 476)	Test (n = 1,051)	Total (n = 4,903)
Extraction difficulty				
Maxillary				
VE	1,282	161	447	1,890
STI	1,613	222	428	2,263
CBI	1,459	239	505	2,203
Mandibular				
VE	267	27	74	368
STI	145	26	38	209
PBI	1,292	174	417	1,883
CBI	4,291	629	1,336	6,256
Complication				
Sinus perforation				
Low	577	57	158	792
Medium	3,516	512	1,143	5,171
High	261	53	79	393
IAN Injury				
Low	990	136	227	1,353
Medium	4,190	604	1,348	6,142
High	815	116	290	1,221

Table 1. Numbers of third molar distributed in each class of extraction difficulty and complication.

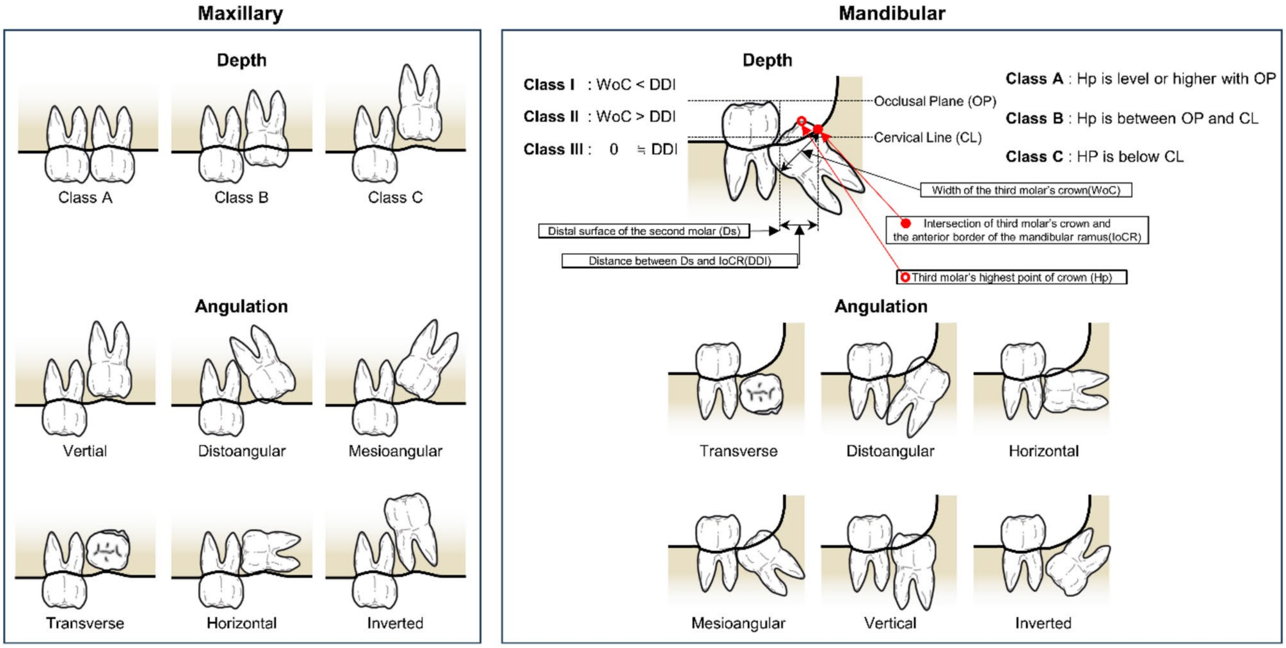

Fig. 2. Illustration of impaction types of maxillary and mandibular third molar based on Pell & Gregory and Winter's classifications.

Depth	Angle	Extraction difficulty	Depth	Angle	Extraction difficulty	Depth	Angle	Extraction difficulty
A	V	VE	B	V	STI	C	V	CBI
A	M	STI	B	M	STI	C	M	CBI
A	H	CBI	B	H	CBI	C	H	CBI
A	D	VE	B	D	STI	C	D	CBI
A	T	STI	B	T	CBI	C	T	CBI
A	I	-	B	I	-	C	I	CBI

Table 2. Extraction difficulty of the impacted maxillary third molar (VE, STI, and CBI). Combinations of the depth (Class A, B, and C) and angle of the impacted maxillary third molar. The angle of the impacted third molar: vertical (V), mesiangular (M), horizontal (H), distoangular (D), transverse (T), and inverted (I).

Deep learning model

As shown in Fig. 1, our deep learning model comprises two stages. The segmentation stage predicts the area of the M3 s, second molars, maxillary sinuses, and IAC. The classification stage predicts the extraction difficulty of maxillary and mandibular M3 s, sinus perforation, and IAN injury possibilities.

We used Deeplabv3+, one of the best-performing models in image segmentation, to segment the M3 s, second molars, maxillary sinuses, and IAC in the OPGs. Deeplabv3 + has an encoder-decoder architecture with atrous convolution and atrous spatial pyramid pooling (ASPP)[28]. OPGs vary due to resolution, viewing angle of various panoramic X-ray equipment, and the patient's movement during imaging. The input images were resized to 2,048 × 1,024 and augmented with a random crop, random flip, and photometric distortion to achieve robust performance against variations. Additionally, contrast limit adaptive histogram equalization (CLAHE) was applied to increase the contrast of the input images[29]. The model was trained using the stochastic gradient descent (SGD) optimizer with a learning rate of 0.01, batch size of 8, and cross-entropy loss. The semantic mask was generated by segmenting the M3 s, second molars, maxillary sinuses, and IAC. Moreover, the region of interest (RoI) with the M3 and the surrounding area was extracted from the OPG with a size of 700 × 700 pixels. The maxillary RoI included the maxillary M3, second molar, and maxillary sinus, whereas the mandibular RoI included the mandibular M3, second molar, and IAC.

We used an R50 + Vision transformer, a hybrid model of Vision transformer, and ResNet-50 to predict the extraction difficulty of the maxillary and mandibular M3 s and the possibility of sinus perforation and IAN injury after extraction[30,31]. The classification model was modified by adjusting the number of channels in the first convolution layer to allow the input of both the RoI and the semantic mask, which is the output of the segmentation model. The models were pretrained on an ImageNet dataset[32]. The models were trained using RoI with a semantic mask to improve classification performance. The input images were resized to 384 × 384 and used in augmentation such as random rotation (– 30 ° to 30 °) and horizontal flip to minimize the model's bias

Depth	Distance	Angle	Extraction difficulty	Depth	Distance	Angle	Extraction difficulty	Depth	Distance	Angle	Extraction difficulty
A	I	V	VE	B	I	V	STI	C	I	V	CBI
A	I	M	PBI	B	I	M	CBI	C	I	M	CBI
A	I	H	PBI	B	I	H	CBI	C	I	H	CBI
A	I	D	STI	B	I	D	STI	C	I	D	CBI
A	I	T	PBI	B	I	T	CBI	C	I	T	CBI
A	I	I	CBI	B	I	I	CBI	C	I	I	CBI
A	II	V	STI	B	II	V	CBI	C	II	V	CBI
A	II	M	PBI	B	II	M	CBI	C	II	M	CBI
A	II	H	PBI	B	II	H	CBI	C	II	H	CBI
A	II	D	PBI	B	II	D	CBI	C	II	D	CBI
A	II	T	CBI	B	II	T	CBI	C	II	T	CBI
A	II	I	CBI	B	II	I	CBI	C	II	I	CBI
A	III	V	CBI	B	III	V	CBI	C	III	V	CBI
A	III	M	CBI	B	III	M	CBI	C	III	M	CBI
A	III	H	CBI	B	III	H	CBI	C	III	H	CBI
A	III	D	CBI	B	III	D	CBI	C	III	D	CBI
A	III	T	CBI	B	III	T	CBI	C	III	T	CBI
A	III	I	CBI	B	III	I	CBI	C	III	I	CBI

Table 3. Extraction difficulty of the impacted mandibular third molar (VE, STI, PBI, and CBI). Combinations of the depth, angle of the mandibular third molar, and distance between the mandibular third molar and the ascending mandibular Ramus (Class I, II, and III).

in the training process. The models were trained using an Adam optimizer with a learning rate of 0.0001, batch size of 8, and cross-entropy loss.

Statistical analysis and evaluation metrics

Segmentation and classification performance were evaluated using various metrics. For segmentation, the metrics included pixel accuracy, precision, recall, dice coefficient, and Intersection over Union (IoU). Pixel accuracy measures the ratio of correctly classified pixels. Precision (TP/(TP + FP)) and recall (TP/(TP + FN)) depend on true positives (TP), false positives (FP), true negatives (TN), and false negatives (FN). The dice coefficient, calculated as 2 TP/(2 TP + FP + FN), represents the harmonic mean of precision and recall. The Jaccard index measures the overlap between ground truth and prediction areas.

For classification, metrics included accuracy, F1-score, specificity, sensitivity, and area under the receiver operating characteristic curve (AUROC). Accuracy is the ratio of correct predictions. Specificity (TN/(TN + FN)) measures the proportion of negatives correctly identified. Sensitivity (TP/(TP + FN)), synonymous with recall, measures the proportion of positives correctly identified. AUROC evaluates the model's performance across various thresholds.

Results

Table 4 shows the segmentation performance for 13 classes: background, M3 s (#18, #28, #38, #48), second molars (#17, #27, #37, #47), maxillary sinuses (right and left), and IAC (right and left). The segmentation performance shows over 90% in pixel accuracy, precision, recall, and dice coefficient and over 80% in IoU. However, the segmentation performance of IAC is 70—80% in four evaluation metrics and less than 60% in IoU. Because, it is challenging to recognize IAC as it is nonclear in the OPG. The segmentation results are visualized in the OPG in Fig. 3.

Table 5 shows the classification performance of the extraction difficulty of the maxillary and mandibular M3 and the possibility of sinus perforation and IAN injury. We compared the model's performance using only RoI as input and the model using RoI and the semantic mask. The experimental results showed that mask-guided attention aids performance improvement. Performance for sinus perforation and extraction difficulty possibilities of the mandibular M3 increased to approximately 7% and 4% in terms of accuracy and approximately 9% and 6% in terms of the F1-score. However, the AUROC for the possibility of sinus perforation decreased from 91.91 to 91.78%. For extraction difficulty and possibility of complications, we achieved accuracy, F1-score, and AUROC scores of 87.97—91.45%, 79.04—87.75%, and 91.91—97.30%, respectively. Figure 3 shows the confusion matrix of the four classifications to determine the labels that the model confused for each class.

Discussion

Diagnostic support technologies related to third molar extraction have been continuously researched, but there is a need for further development to provide greater convenience to clinicians. Many studies have proposed methods for predicting the extraction difficulty of mandibular M3 using deep learning models on OPGs. For instance, there have been studies focused on classifying the extraction difficulty of mandibular M3 s or classifying the relationship between the mandibular M3 and the IAC[17,19–21,23–25]. One study has also proposed

Class	Pixel accuracy, %	Precision, %	Recall, %	Dice coefficient (F1-score), %	IoU (Jaccard index), %
Background	98.53	98.87	98.53	98.70	97.43
Third molar					
#18	87.72	92.69	87.72	90.14	82.04
#28	91.45	89.04	91.45	90.23	82.20
#38	92.28	92.64	92.28	92.46	85.98
#48	90.55	93.88	90.55	92.18	85.50
Second molar					
#17	89.42	91.32	89.42	90.36	82.41
#27	91.96	88.64	91.96	90.27	82.27
#37	92.08	92.06	92.08	92.07	85.31
#47	92.14	91.77	92.14	91.96	85.11
Maxillary sinus					
Rt.Sinus	90.88	91.61	90.88	91.25	83.90
Lt.Sinus	95.22	87.75	95.22	91.33	84.05
IAC					
Rt.Canal	70.21	77.30	70.21	73.58	58.21
Lt.Canal	72.20	77.03	72.20	74.54	59.41
Average	**88.82**	**89.59**	**88.83**	**89.16**	**81.06**

Table 4. Segmentation performance of third molars, second molars, maxillary sinuses, and IAC in the OPGs.

methods for evaluating the extraction difficulty of maxillary M3 s using deep learning models[18]. However, most previous research has focused on either mandibular or maxillary M3 s individually. In practice, it is essential to evaluate the extraction difficulty for both maxillary and mandibular M3 s and analyze the relationships between the maxillary M3 and the maxillary sinus, as well as the mandibular M3 and the IAC. To address this, we propose a method that predicts both the extraction difficulty and the relationships for all these structures, including both maxillary and mandibular M3 s, the maxillary sinus, and the IAC.

While existing methods typically detect M3 s first and then classify extraction difficulty based on the detected M3 s, our model adopts a different approach[19,20,23,24]. We first segment the maxillary and mandibular M3 s, the maxillary sinus, and the IAC, and use the segmented masks as inputs for the classification model, thereby enhancing the classification performance. This approach not only improves performance but also introduces a technique that enhances the model's capability, rather than simply applying the existing classification model.

Our dataset comprised 4,903 OPGs acquired using eight dental panoramic imaging devices at 13 hospitals. Therefore, OPGs have distinctions, such as illuminance and resolution. Considering that the OPGs were acquired from many patients, they included diverse materials such as prosthodontics, endodontics, and resin. The differences and the presence of various materials can decrease diagnostic performance. Nevertheless, as shown in Table 5, the proposed deep learning model diagnosed the extraction difficulty and possible complications with high performance. We achieved accuracy and AUROC of over 87% and 96% for classifying extraction difficulty and over 88% and 91% for possibility of complications, respectively. As a result, our deep learning model demonstrated consistent high performance when applied to various patients in hospitals using different devices.

As shown in the classification in Fig. 1, we maximized the classification performance by using the RoI of the OPG and the semantic mask as inputs. Table 5shows that the classification performance improved in terms of the evaluation metrics when both the OPG and semantic mask were used. In particular, performance increased significantly in classifying possible complications. Since the maxillary sinus and IAC are dimmed in the OPG, they are highlighted using the semantic mask. The prediction performance for possible complications, where the sinus and IAC are crucial factors, significantly improved[34]. Previous studies support the improvement of classification performance through a semantic mask. For lesion classification, the dermoscopic image and a lesion-semantic mask generated by segmenting skin lesions in the dermoscopic image were used to achieve more than 90% in AUC[35]. Additionally, collaborative learning was used for lesion segmentation and disease severity classification to diagnose diabetic retinopathy in fundus images[36].

We used RoI instead of the original OPG as input to the classification model. Since an OPG is a high-resolution image, it requires a significant amount of computing resources and computation time. Therefore, using a smaller RoI as an input reduced memory and computation resources. Because the RoI contains sufficient information for diagnosis, both efficiency and effectiveness were achieved.

This study employed the most extensive dataset compared to previous studies that applied deep learning to diagnose dental diseases. We classified VE, STI, and CBI, as there were no data on the PBI of maxillary M3 s within our dataset. It is necessary to generalize and improve further diagnostic performance by introducing more diverse patient data.

In conclusion, this study proposed a novel method for diagnosing the extraction difficulty of M3 s and the possible complications after extraction using deep neural networks. The proposed method showed that automatic diagnosis via deep learning is sufficiently feasible, and high performance can be achieved. Using OPGs

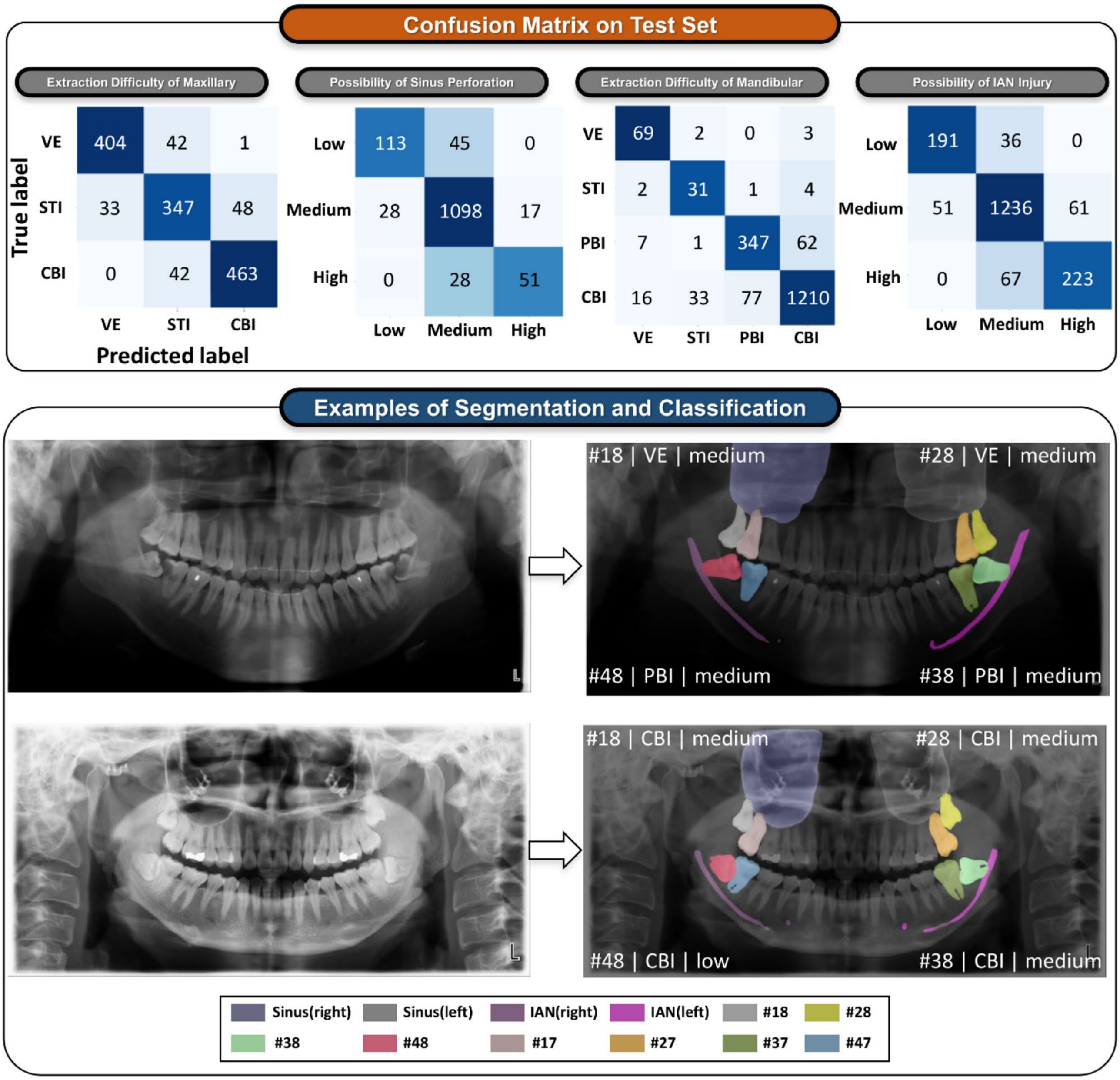

Fig. 3. **(Confusion Matrix on Test Set)** The confusion matrix shows correctly and wrongly classified test samples. The confusion matrix displays correctly classified samples along the diagonals and incorrectly classified samples along the off-diagonal elements. **(Examples of Segmentation and Classification)** Examples of segmentation and classification results on the test set. Left: original OPGs. Right: OPGs reflecting the results of segmentation and classification. The segmentation results of the third molars (#18, #28, #38, #48), second molars (#17, #27, #37, #47), maxillary sinus (left and right), and IAC (left and right) are expressed in different colors for each instance. The classification results are expressed in white in the order of tooth number, the extraction difficulty, and the possibility of complication.

and semantic masks generated through segmentation effectively improved diagnostic performance. We expect that our study can be used to support clinicians.

	Accuracy %	F1-score %	Specificity %	Sensitivity %	AUROC %
Extraction difficulty					
Maxillary					
OPG w/o semantic mask	85.87	85.98	86.08	93.13	96.08
OPG with semantic mask (ours)	**87.97**	**87.75**	**87.71**	**94.01**	**96.25**
Sinus perforation					
OPG w/o semantic mask	84.93	70.44	77.38	87.09	91.91
OPG with semantic mask (ours)	**91.45**	**79.96**	**77.39**	**88.53**	91.78
Mandibular					
Extraction difficulty					
OPG w/o semantic mask	84.93	73.46	76.89	96.41	95.71
OPG with semantic mask (ours)	**88.85**	**79.04**	**78.15**	94.55	**97.30**
IAN Injury					
OPG w/o semantic mask	85.52	79.63	81.26	93.48	93.47
OPG with semantic mask (ours)	**88.47**	**83.72**	**84.24**	91.03	**94.13**

Table 5. Classification performance of extraction difficulty and possibility of sinus perforation and IAN injury.

Data availability
The data generated and analyzed in this study are not publicly available due to privacy laws and regulations in Korea, but they can be obtained from the corresponding author upon reasonable request.

Received: 22 July 2024; Accepted: 25 April 2025
Published online: 30 May 2025

References
1. Hugoson, A. & Kugelberg, C. F. The prevalence of third molars in a Swedish population. An epidemiological study. *Community Dent. Health*. **5**, 121–138 (1988).
2. Gisakis, I. G., Palamidakis, F. D., Farmakis, E. T. R., Kamberos, G. & Kamberos, S. Prevalence of impacted teeth in a Greek population. *J. Investig Clin. Dent.* **2**, 102–109 (2011).
3. Kim, H. J. et al. Anatomical risk factors of inferior alveolar nerve injury association with surgical extraction of mandibular third molar in Korean population. *Appl. Sci.* **11**, 816 (2021).
4. Rothamel, D. et al. Incidence and predictive factors for perforation of the maxillary antrum in operations to remove upper wisdom teeth: prospective multicentre study. *Br. J. Oral Maxillofac. Surg.* **45**, 387–391 (2007).
5. Sarikov, R. & Juodzbalys, G. Inferior alveolar nerve injury after mandibular third molar extraction: a literature review. *J. Oral Maxillofac. Res.* **5**, e1 (2014).
6. Hasegawa, T. et al. Risk factors associated with Oroantral perforation during surgical removal of maxillary third molar teeth. *Oral Maxillofac. Surg.* **20**, 369–375 (2016).
7. Deliverska, E. G. & Petkova, M. Complications after extraction of impacted third molars-literature review. *J. IMAB-Annu Proc. Sci.* **22**, 1202–1211 (2016).
8. Chow, H. T. & Teh, L. Y. Sensory impairment after resection of the mandible: a case report of 10 cases. *J. Oral Maxillofac. Surg.* **58**, 629–635 (2000).
9. Kjølle, G. K. & Bjørnland, T. Low risk of neurosensory dysfunction after mandibular third molar surgery in patients less than 30 years of age. A prospective study following removal of 1220 mandibular third molars. *Oral Surg. Oral Med. Oral Pathol. Oral Radiol.* **116**, 411–417 (2013).
10. Yalçın, S., Öncü, B., Emes, Y., Atalay, B. & Aktaş, İ. Surgical treatment of Oroantral fistulas: a clinical study of 23 cases. *J. Oral Maxillofac. Surg.* **69**, 333–339 (2011).
11. Iizuka, T., Tanner, S. & Berthold, H. Mandibular fractures following third molar extraction: a retrospective clinical and radiological study. *Int. J. Oral Maxillofac. Surg.* **26**, 338–343 (1997).
12. Lim, A. A. T., Wong, C. W. & Allen, J. C. Jr Maxillary third molar: patterns of impaction and their relation to Oroantral perforation. *J. Oral Maxillofac. Surg.* **70**, 1035–1039 (2012).
13. Yilmaz, S., Adisen, M. Z., Misirlioglu, M. & Yorubulut, S. Assessment of third molar impaction pattern and associated clinical symptoms in a central Anatolian Turkish population. *Med. Princ Pract.* **25**, 169–175 (2016).
14. Chen, L. et al. DRINet for medical image segmentation. *IEEE Trans. Med. Imaging.* **37**, 2453–2462 (2018).
15. Shin, S. et al. Rapid and non-destructive spectroscopic method for classifying beef freshness using a deep spectral network fused with myoglobin information. *Food Chem.* **352**, 129329 (2021).
16. Huang, S. C., Le, T. H. & Jaw, D. W. DSNet: joint semantic learning for object detection in inclement weather conditions. *IEEE Trans. Pattern Anal. Mach. Intell.* **43**, 2623–2633 (2020).
17. Milani, O. H. et al. A fully automated classification of third molar development stages using deep learning. *Sci. Rep.* **14**, 13082 (2024).
18. Torul, D., Akpinar, H., Bayrakdar, I. S., Celik, O. & Orhan Kaan. Prediction of extraction difficulty for impacted maxillary third molars with deep learning approach. *J. Stomatol. Oral Maxillofac. Surg.* **125**, 101817 (2024).
19. Soltani, P. et al. A two-stage deep-learning model for determination of the contact of mandibular third molars with the mandibular Canal on panoramic radiographs. *BMC Oral Health*. **24**, 1373 (2024).
20. Trachoo, V. et al. Deep learning for predicting the difficulty level of removing the impacted mandibular third molar. *Int. Dent. J.* (2024).
21. Kumbasar, N., Guller, M. T., Miloglu, O., Oral, E. A. & Ozbek, I. Y. Deep-learning based fusion of Spatial relationship classification between mandibular third molar and inferior alveolar nerve using panoramic radiograph images. *Biomed. Signal. Process. Control.* **100**, 107059 (2025).

22. Park, J., Lee, J., Moon, S. & Lee, K. Deep learning based detection of missing tooth regions for dental implant planning in panoramic radiographic images. *Appl. Sci.* **12**, 1595 (2022).
23. Yoo, J. H. et al. Deep learning based prediction of extraction difficulty for mandibular third molars. *Sci. Rep.* **11**, 1954 (2021).
24. Lee, J., Park, J., Moon, S. Y. & Lee, K. Automated prediction of extraction difficulty and inferior alveolar nerve injury for mandibular third molar using a deep neural network. *Appl. Sci.* **12**, 475 (2022).
25. Sukegawa, S. et al. Evaluation of multi-task learning in deep learning-based positioning classification of mandibular third molars. *Sci. Rep.* **12**, 684 (2022).
26. Pell, G. J. Impacted mandibular third molars: classification and modified techniques for removal. *Dent. Digest.* **39**, 330–338 (1933).
27. Winter, G. B. *Impacted Mandibular Third Molars*79 (American Medical Book Co, 1926).
28. Chen, L. C., Zhu, Y., Papandreou, G., Schroff, F. & Adam, H. Encoder-decoder with atrous separable convolution for semantic image segmentation, in Proceeding of the European conference on computer vision, 801–818 (2018).
29. Reza, A. M. Realization of the contrast limited adaptive histogram equalization (CLAHE) for real-time image enhancement. *J. VLSI Signal. Process. Syst. Signal. Image Video Technol.* **38**, 35–44 (2004).
30. He, K., Zhang, X., Ren, S. & Sun, J. Deep residual learning for image recognition. in Proceedings of the IEEE conference on computer vision and pattern recognition, 770–778 (2016).
31. Dosovitskiy, A. et al. An image is worth 16x16 words: transformers for image recognition at scale. arXiv preprint arXiv:2010.11929 (2020).
32. Deng, J. et al. Imagenet: a large-scale hierarchical image database. in Proceedings of the IEEE conference on computer vision and pattern recognition, 248–255 (2009).
33. Shin, S., Lee, J., Lee, J., Yu, Y. & Lee, K. Teaching where to look: attention similarity knowledge distillation for low resolution face recognition. in Proceeding of the European conference on computer vision, 631–647 (2022).
34. Choi, E. et al. Artificial intelligence in positioning between mandibular third molar and inferior alveolar nerve on panoramic radiography. *Sci. Rep.* **12**, 2456 (2022).
35. Xie, Y., Zhang, J., Xia, Y. & Shen, C. A mutual bootstrapping model for automated skin lesion segmentation and classification. *IEEE Trans. Med. Imaging.* **39**, 2482–2493 (2020).
36. Zhou, Y. et al. Collaborative learning of semi-supervised segmentation and classification for medical images. in Proceedings of the IEEE/CVF conference on computer vision and pattern recognition. 2079–2088 (2019).
37. Khojastepour, L., Khaghaninejad, M. S., Hasanshahi, R., Forghani, M. & Ahrari, H. Does the winter or pell and Gregory classification system indicate the apical position of impacted mandibular third molars? *J. Oral Maxillofac. Surg.* **77**, 2222e1–2222e9 (2019).
38. Santos, K. K., Lages, F. S., Maciel, C. A. B., Gloria, J. C. R. & Oliveira, D. W. Prevalence of mandibular third molars according to the pell & Gregory and winter classifications. *J. Oral Maxillofac. Surg.* 1–7 (2022).

Acknowledgements

This work was supported by the Development of a Situational Awareness System for Preventing Collisions and Accidents of Autonomous Ship (20011722) funded by the Ministry of Trade, Industry & Energy (MOTIE) and Korea Planning & Evaluation Institute of Industrial Technology (KEIT).

Author contributions

All authors gave their fnal approval and agreed to be accountable for all aspects of the work.J.L. contributed to conception, design, data acquisition, analysis, and interpretation, drafted and critically revised the manuscript. J.P, S.L contributed to design, data analysis, and interpretation, drafted and critically revised the manuscript. S.Y.M. contributed to conception, and data acquisition, drafted and critically revised the manuscript; K.L. contributed to conception, design, data acquisition, analysis, and interpretation, drafted and critically revised the manuscript.

Declarations

Competing interests

The authors declare no competing interests.

Code availability

The code for implementing this project is open-sourced at https://github.com/gist-ailab/man-max-third-molar.

Additional information

Correspondence and requests for materials should be addressed to K.L.